(Distribution Restricted)
until February 16, 1986

Crustal Structure of the Green Canyon Area, Northern Gulf of Mexico: An Ocean-Bottom Seismograph - Air Gun Experiment

by

Yosio Nakamura, Dale S. Sawyer, Joseph O. Ebeniro,
William P. O'Brien, Jr., F. Jeanne Shaub and Jürgen Oberst

Final Report of Research Agreement

Submitted to Sponsor

April 30, 1985

Institute for Geophysics
The University of Texas at Austin
4920 North I.H. 35
Austin, Texas 78751

University of Texas Institute for Geophysics Technical Report No. 38

SUMMARY

We have conducted a large-offset seismic experiment in the Green Canyon area of the northern Gulf of Mexico, offshore of Louisiana, using large-capacity air guns and ocean-bottom seismographs. The purpose of the experiment was to map the deep sedimentary and crustal structures underlying the thick sedimentary cover which also included many salt intrusives. Five lines, each approximately 100 km long with four OBS's, were shot over an area which extended from mid-shelf at about 50 m water depth to just beyond the Sigsbee Escarpment at about 2500 m water depth.

The acquired data were analyzed and interpreted initially using standard techniques: layer solutions from phase velocities and intercept times of refracted arrivals and interval velocities from moveout of wide-angle reflections. For most of the data, however, the structures were too complex to yield much information by these one-dimensional analyses. In these cases, we used two-dimensional ray tracing to define shallow structures as well as the depths to the deeper refractors.

Most of the area except for the extreme northern and southern portions is underlain by relatively shallow detached salt with seismic velocities ranging from 3.5 to 4.5 km/s. Thickness of the salt varies from place to place, but a general trend of its thinning toward the south is noted. The root of the salt, if extant, is seismically indistinguishable from clastic sediments at depth.

On most of the lines, the top of the Challenger unit (i.e. middle Cretaceous unconformity) and the top of the basement are identifiable below the salt. The basement lies at about 15 km depth in most of the study area, but appears to rise to about 12 km depth below the outer slope. The Moho is observed only in the extreme southern part of the area. Basinward of the Sigsbee Escarpment, its depth is about 19 km below sea level, but it deepens to 25 km below the outer slope.

For a better definition of the sub-basement structures below thick sediments that include shallow salt, we need to further improve our data acquisition techniques.

INTRODUCTION

Wide areas of the northern Gulf of Mexico are underlain by thick sediments transported from the vast expanse of the North American continent since early Cretaceous time. Because of this thick sedimentary cover and also of numerous salt deposits that are found in many areas of this region, it is difficult, and often impossible, to probe the underlying crustal layers using seismic reflection techniques commonly used in the petroleum industry.

In order to acquire seismic data relevant to the deep crustal structure of the northern Gulf of Mexico, we have been conducting a series of large-offset seismic experiments using ocean-bottom seismographs (OBS) and large-capacity air-gun sources. The use of OBS allows us to extend seismic lines to very large offsets, thus enabling us to obtain refracted and wide-angle reflected arrivals from deep layers. The relative quiescence of the ocean floor compared with the sea surface is also advantageous for detection of weak seismic signals. Air-gun sources provide more accurately timed, uniform and spatially denser sources than conventional explosive sources commonly used in similar seismic refraction surveys.

This report covers the results of an experiment conducted in early 1984 in the Green Canyon area off the Louisiana coast, Fig. 1.

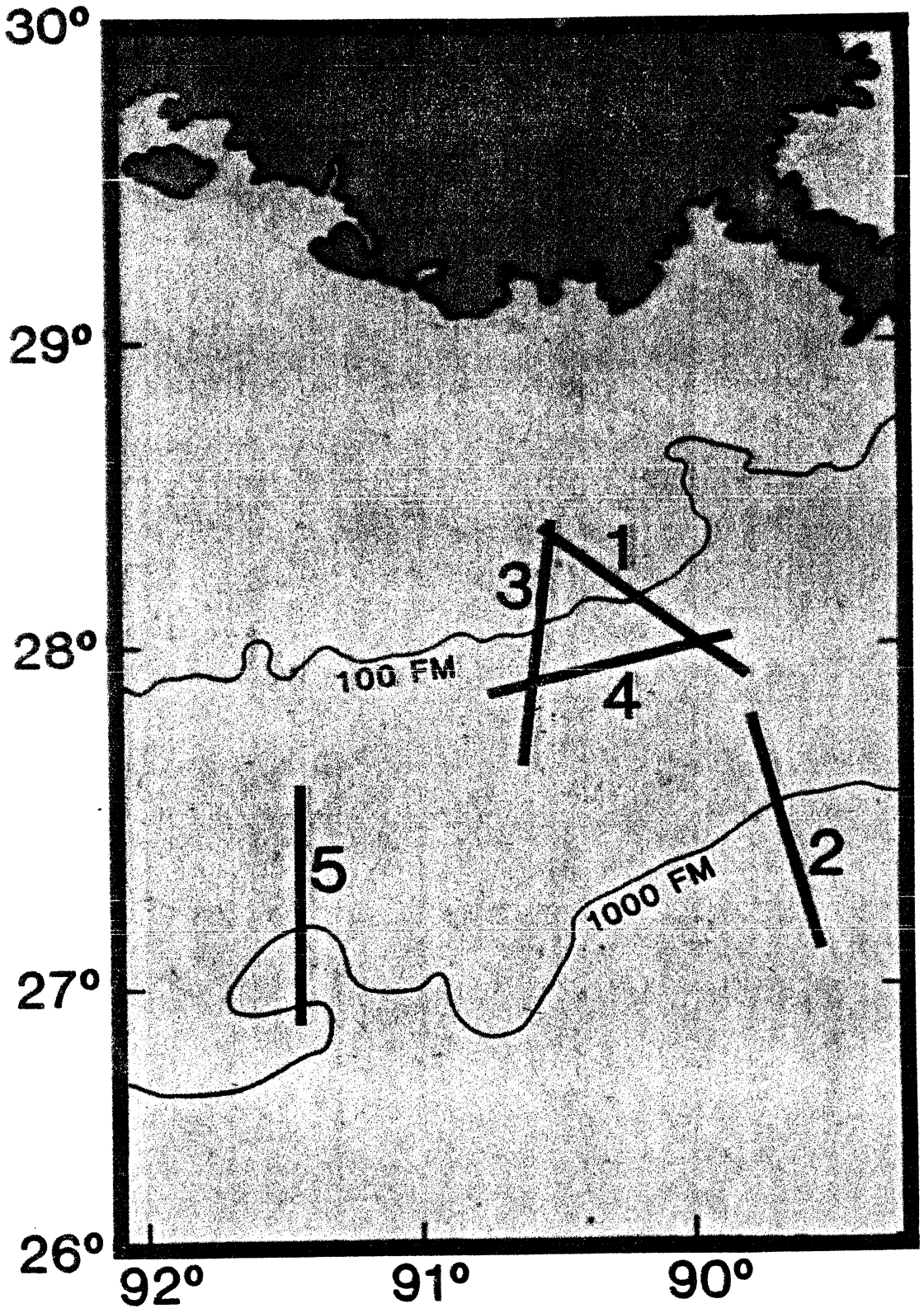

Fig. 1. Location map of the five seismic lines shot during the experiment.

FIELD EXPERIMENT

Seismic Lines

The five seismic lines, Fig. 1, were selected by the sponsor. Each line is approximately 100 km long with four OBS's as receivers and 1081 air-gun shots as signal sources along each line. Additionally, a few sonobuoys were also deployed on each line for supplementary information. Coordinates of the line end points and locations of the successful OBS's are listed in Tables 1 and 2, respectively.

The geometry of the seismic lines, Fig. 2, is different from that of normal seismic reflection lines because of the fixed receiver locations. With each OBS not being tied to the shooting ship, a wide range of offsets, from practically zero to nearly the entire length of the line, can be achieved. This allows detection of near-vertical reflections as well as wide-angle reflections and refractions from deep layers. We deployed one OBS near each end and one at about 20 km from each end. This assured a maximum offset of at least 70 km for all OBS's. The sonobuoys filled in the wide gap between the two inner OBS's.

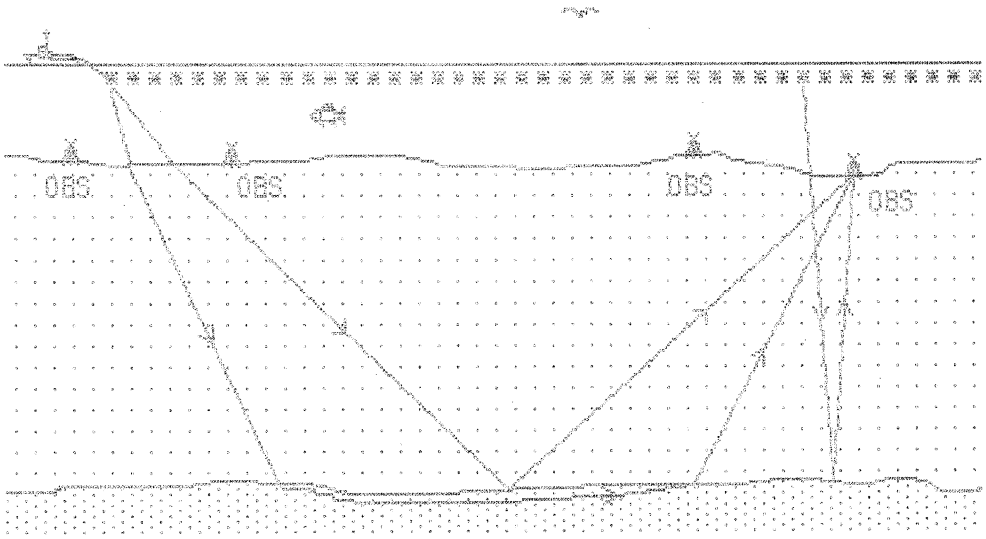

Fig. 2. Geometry of seismic line with four OBS's

Instrumentation

The ocean-bottom seismograph used for this experiment is a very sophisticated seismograph package developed at the University of Texas for detection of seismic signals at the ocean floor. It is an integrated package consisting of the following components: a) a sensor system; b) a set of three preamplifiers; c) a set of three binary-gain-ranging amplifiers; d) a 3-channel signal multiplexer; e) a 12-bit analog-to-digital converter; f) up to 96K bytes of temporary data storage memory; g) a digital cartridge tape recorder; h) a clock; i) an acoustic transponder; j) a release mechanism; and k) a set of recovery aids.

Table 1. End coordinates of seismic lines

Line	Shot 1		Shot 1081	
1	27°53.80' N	89°47.01' W	28°25.61' N	90°34.35' W
2	27°48.30' N	89°47.08' W	26°56.82' N	89°31.14' W
3	28°25.53' N	90°29.00' W	27°32.69' N	90°36.10' W
4	28°02.46' N	89°45.42' W	27°49.62' N	90°47.38' W
4R	27°49.83' N	90°45.62' W	28°02.69' N	89°47.44' W
5	27°35.06' N	91°26.01' W	26°38.37' N	91°26.63' W

4R: Line 4 reshoot

Table 2. OBS locations

Line	OBS	Latitude	Longitude	Depth, m
1	1	28°22.88' N	90°29.75' W	49
	2	28°16.33' N	90°20.14' W	75
	3	28°01.55' N	89°58.22' W	570
	4	27°54.90' N	89°48.63' W	765
2	1	26°59.97' N	89°32.33' W	2469
	3	27°33.86' N	89°42.84' W	1094
	4	27°44.29' N	89°46.06' W	1011
3	1	27°36.74' N	90°35.53' W	1131
	2	27°47.59' N	90°34.21' W	852
	3	28°11.71' N	90°31.17' W	87
	4	28°22.46' N	90°29.90' W	51
4	1	27°50.76' N	90°41.40' W	783
4R	5	28°01.74' N	89°51.62' W	702
	6	27°59.13' N	90°03.46' W	609
	7	27°55.29' N	90°21.14' W	694
	8	27°53.27' N	90°30.14' W	583
5	1	26°44.63' N	91°26.33' W	1816
	2	26°55.55' N	91°25.96' W	2257
	3	27°19.94' N	91°25.68' W	1263
	4	27°30.74' N	91°25.61' W	950

The sensor system is normally made up of one to three geophones, but may include a hydrophone. The binary gain ranging permits a wide dynamic range of over 96 dB. The temporary data storage memory, which is enough to store 48,000 12-bit data words, each with sign, exponent and component identification, is required because the tape recorder must be off during data acquisition to avoid vibration noise.

The data acquisition is controlled by three microprocessors for overall system control, clock control and tape recorder control. They are individually programmed to give wide flexibility in data acquisition mode (such as number of channels, sampling interval, record length and timing of recording), compensation of clock drift, formatting of data for recording, and release of the package from the ocean floor.

The electronics subsystems, geophones, the acoustic transponder and strobe lights for recovery aid are contained in a glass sphere, 17 inches in diameter, which fits snugly into a molded plastic cap. The sphere with its contents, the plastic cap, two radio beacons and two orange flags to aid recovery constitute the recovery capsule, the part that is released from the ocean floor after data collection.

On deployment, the recovery capsule is attached firmly to a steel frame footing by three stiff elastic straps, Fig. 3. The frame has many spikes, which penetrate the ocean floor sediments to improve seismic coupling. The release of the package from the ocean floor for surface recovery is accomplished by electrolytically dissolving a stainless steel wire in sea water, and can be controlled in three independent ways: programmed release controlled by the main clock, preset release initiated by a backup clock and surface-ship commanded release through the acoustic transponder.

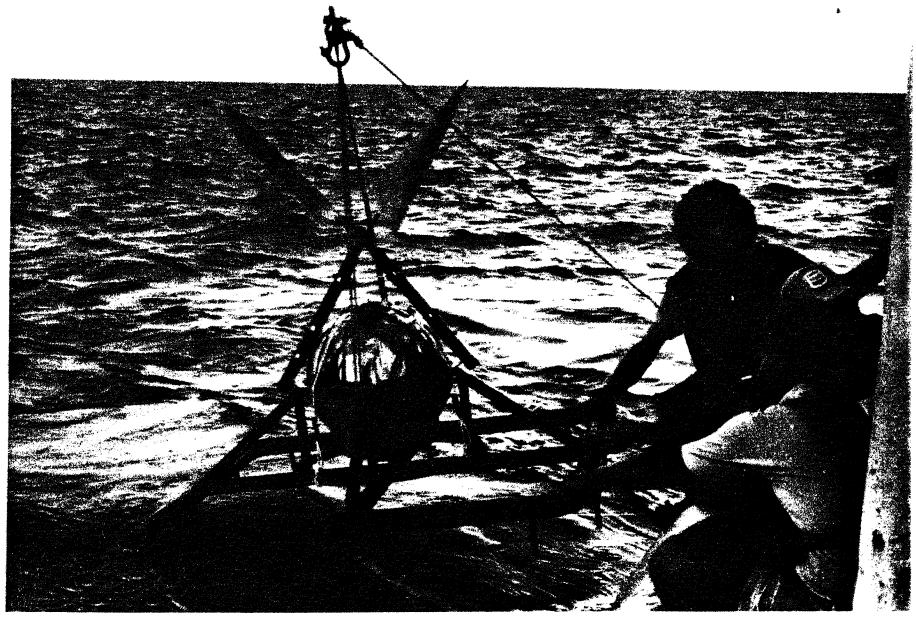

Fig. 3. The Texas OBS being deployed from R/V *Fred H. Moore*.

Field Parameters

Various parameters of the field experiment are listed below:

Source:	Two air guns, Bolt model 800C, 2000 in^3 each, at 2000 psi
Towing depth:	35 feet (11 m)
Repetition rate:	45 sec (30 sec for line extension)
Ship speed:	4 knots
Shot spacing:	93 m (62 m for line extension)
Receiver:	4.5 Hz vertical geophone, Mark Product model L1BU
Pass band:	4.5 - 20 Hz
Overall sensitivity:	7.0×10^{-7} (m/s)/DU
Recording window:	20.4 sec, sliding
Sampling interval:	10.008 ms

Navigation

We used Loran-C as the primary means of navigation to locate each OBS and shot points. Our normal procedure is to use coordinates as determined by satellite navigation to estimate the additional secondary correction factor (ASF) needed for computation of latitude and longitude from the observed Loran-C TD values. However, the doppler sonar was out of order for this cruise and thus the satellite navigation was unreliable. Therefore, for this experiment we used ASF values published in the Loran-C Correction Tables. The ASF values actually used for the computation are listed in Table 3.

Table 3. Loran-C additional secondary correction factors

Line	WASF,μs	XASF,μs
1	-0.2	0.3
2	-0.1	0.3
3	-0.2	0.3
4	-0.2	0.3
5	-0.1	0.3

Since the precision of individual TD readings at each shot was not high enough to compute the relative locations of shot points at high accuracy, the measured TD values were first smoothed using piecewise continuous cubic Hermite functions, and more accurate estimates of TD values at each shot and then shot coordinates were computed from the smoothed TD functions. We estimate the relative distance between shots to be accurate to better than 1%. However, absolute locations may be off by as much as a mile.

Field Experiment

The experiment was conducted from the R/V *Fred H. Moore*, cruise No. FM-22, from the 3rd to the 15th of February, 1984. On each line, four OBS's were deployed at predetermined locations. The line was then retraced while shooting the air guns at 45 second repetition rate for the first 961 shots, or 89 km at 4 knots. An additional 120 shots were fired at 30 second intervals for a 7.4 km extension of the line. We also pulled a short streamer to collect supplementary shallow reflection data at the same time. Finally, the line was retraced for the third time to recover the OBS's.

In all, five lines were shot. However, one of the lines, Line 4, had to be reshot because only one of the four OBS's on the line worked properly for the first shooting. The reshoot with four additional OBS's was successful, and thus data from a total of five OBS locations were acquired for this line. All four OBS's on each of Lines 1, 3 and 5 worked successfully, while one of the four OBS's on Line 5 did not function properly and no data were obtained from this OBS. Thus we collected data from a total of 20 OBS's on five lines during this experiment (Table 2).

DATA PROCESSING

Standard processing of the acquired data consisted of the following steps:

a) Reformatting of the seismic data on cartridge tapes to SEG-Y format: The original OBS data are written on each cartridge tape in a special format to conserve tape usage. The data are reformatted to standard SEG-Y format and are rewritten onto a standard computer tape.

b) Post-cruise recomputation of shot locations: Shot locations are recomputed from the measured Loran-C TD values using the best available ASF values as described above.

c) Location of OBS based on water-wave arrival times: The actual location of each OBS is slightly different from its deployment and recovery locations because of the drift due to existing current and wind. The observed water-wave arrival times are used to determine the actual location of each OBS as well as the exact clock correction at the time of the passage of the shooting ship over the instrument using a least-squares inversion of the arrival times.

d) Merging of navigation data into SEG-Y format tapes: Revised navigation data based on the recomputed shot and OBS locations and clock drift are merged into the initial SEG-Y format tapes described above.

e) 'Stacking' of traces into uniform offset bins: The acquired seismic traces are not evenly spaced in offset because the ship speed varies from time to time while the shooting must be done according to preset time schedule and not by distance. To facilitate interpretation of record sections, we 'stacked' the traces into 100 m bins using a stacking velocity of 6 km/s. The offset range for this stacking was short enough (about ±50 m) so that attenuation of arrivals of phase velocities different from 6 km/s was negligible.

f) Plotting of record sections: The binned traces were plotted to produce the basic seismic record section plots.

The processed products d), e) and f) were then used for further processing and interpretations. Figures 4a through 4e (on fold-out pages) show reduced copies of seismic record sections.

The following figures are on the fold-out pages:

Fig. 4a. Line 1 seismic record sections.

Fig. 4b. Line 2 seismic record sections.

Fig. 4c. Line 3 seismic record sections.

Fig. 4d. Line 4 seismic record sections.

Fig. 4e. Line 5 seismic record sections.

LINE 1

SOUTHEAST

DISTANCE, KM

NORTHWEST

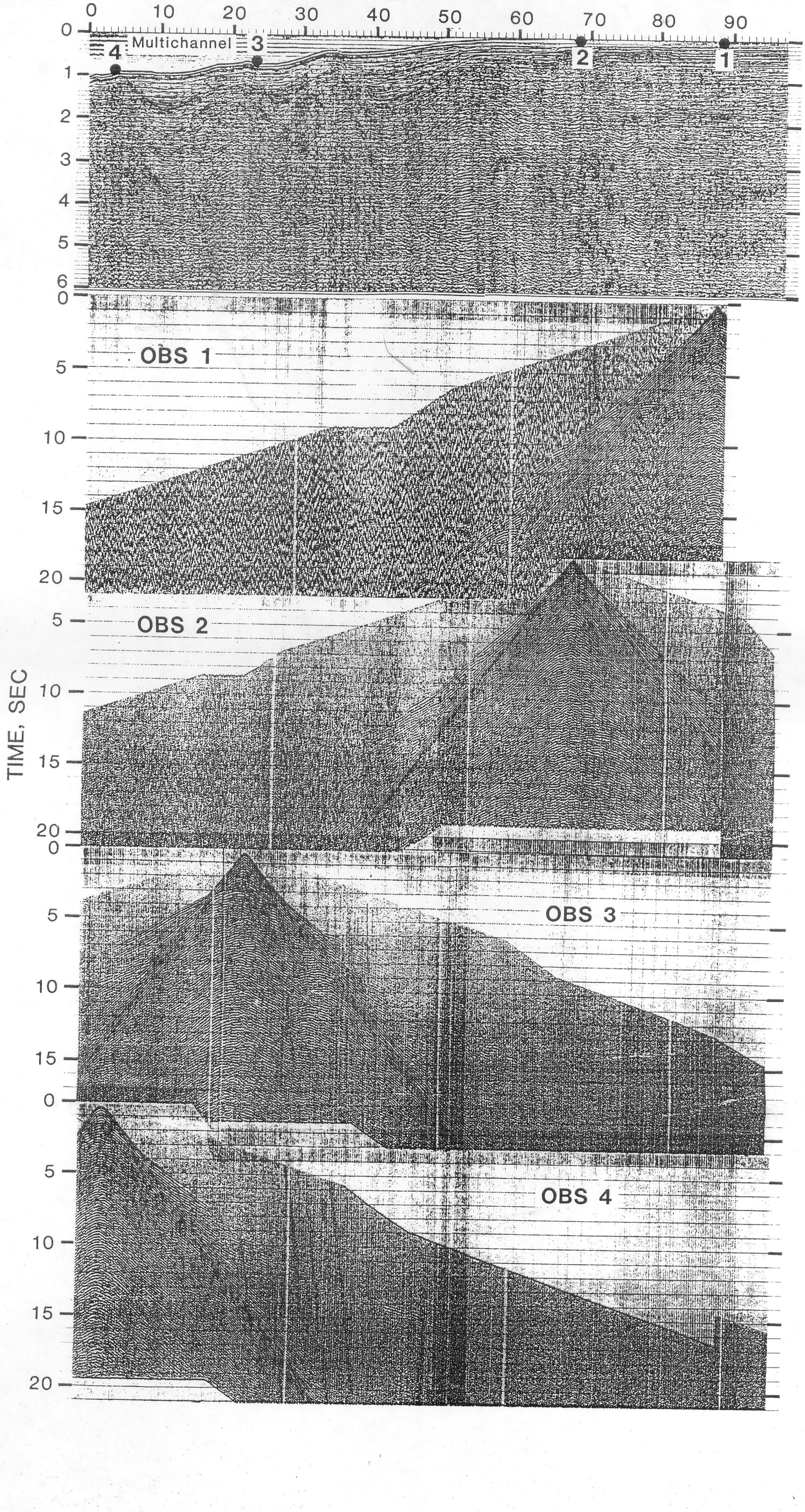

LINE 2

NORTH

SOUTH

DISTANCE, KM

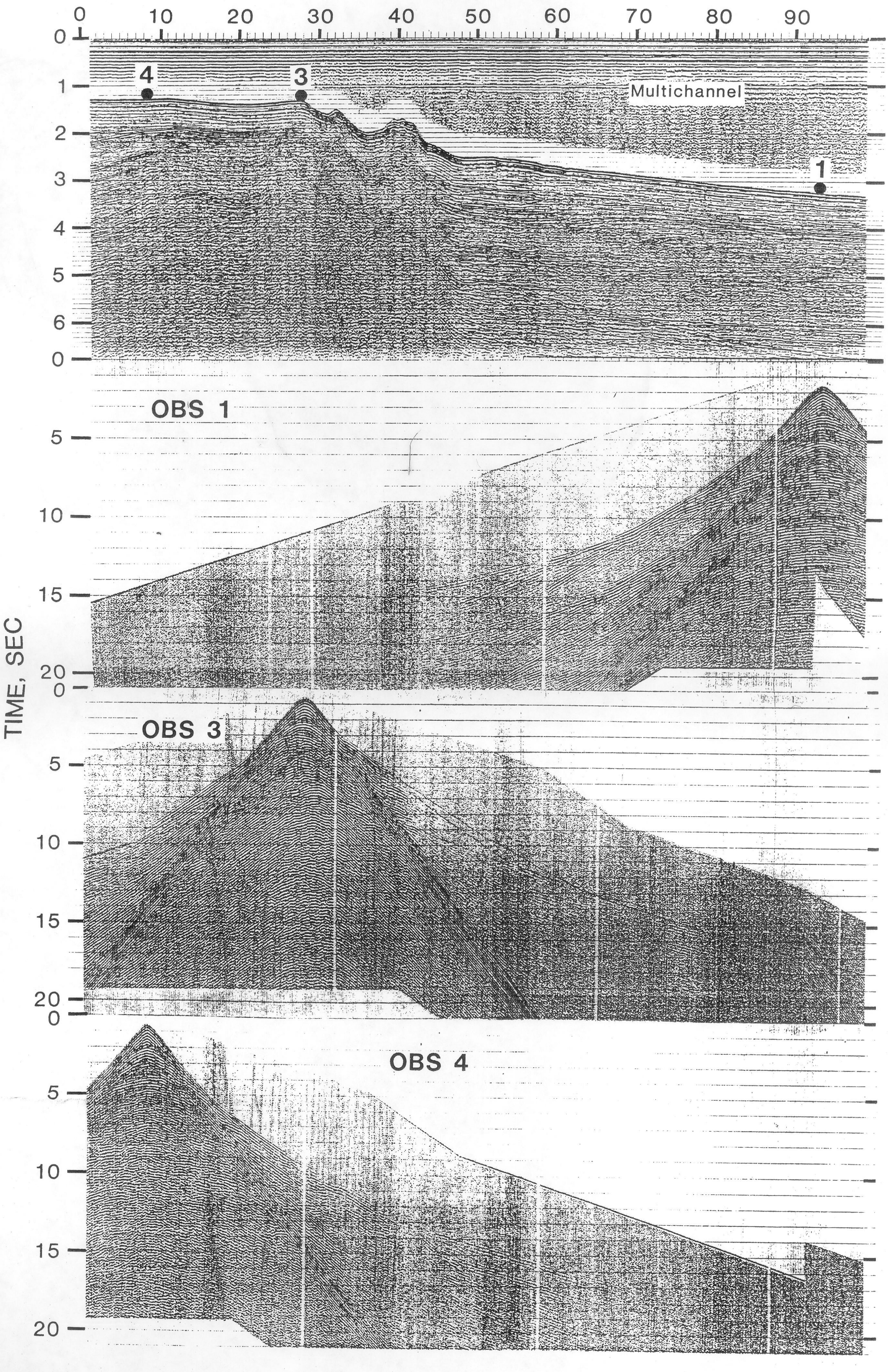

LINE 3

NORTH

SOUTH

DISTANCE, KM

0 10 20 30 40 50 60 70 80 90

4 3 2 1

Multichannel

OBS 1

OBS 2

OBS 3

OBS 4

TIME, SEC

0 5 10 15 20

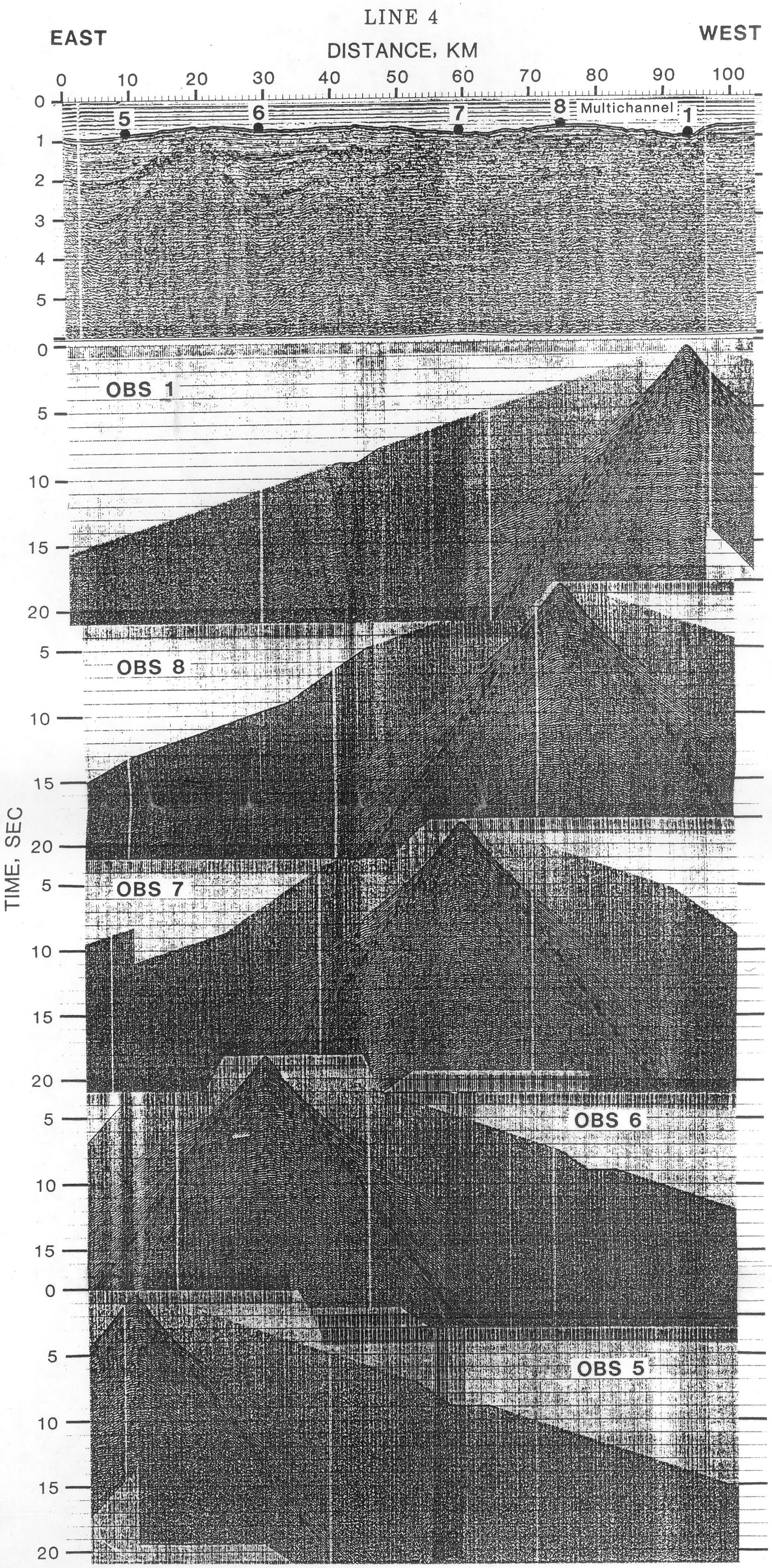
LINE 4
EAST
WEST
DISTANCE, KM
0
10
20
30
40
50
60
70
80
90
100
5
6
7
8
Multichannel
1
OBS 1
OBS 8
OBS 7
OBS 6
OBS 5
TIME, SEC

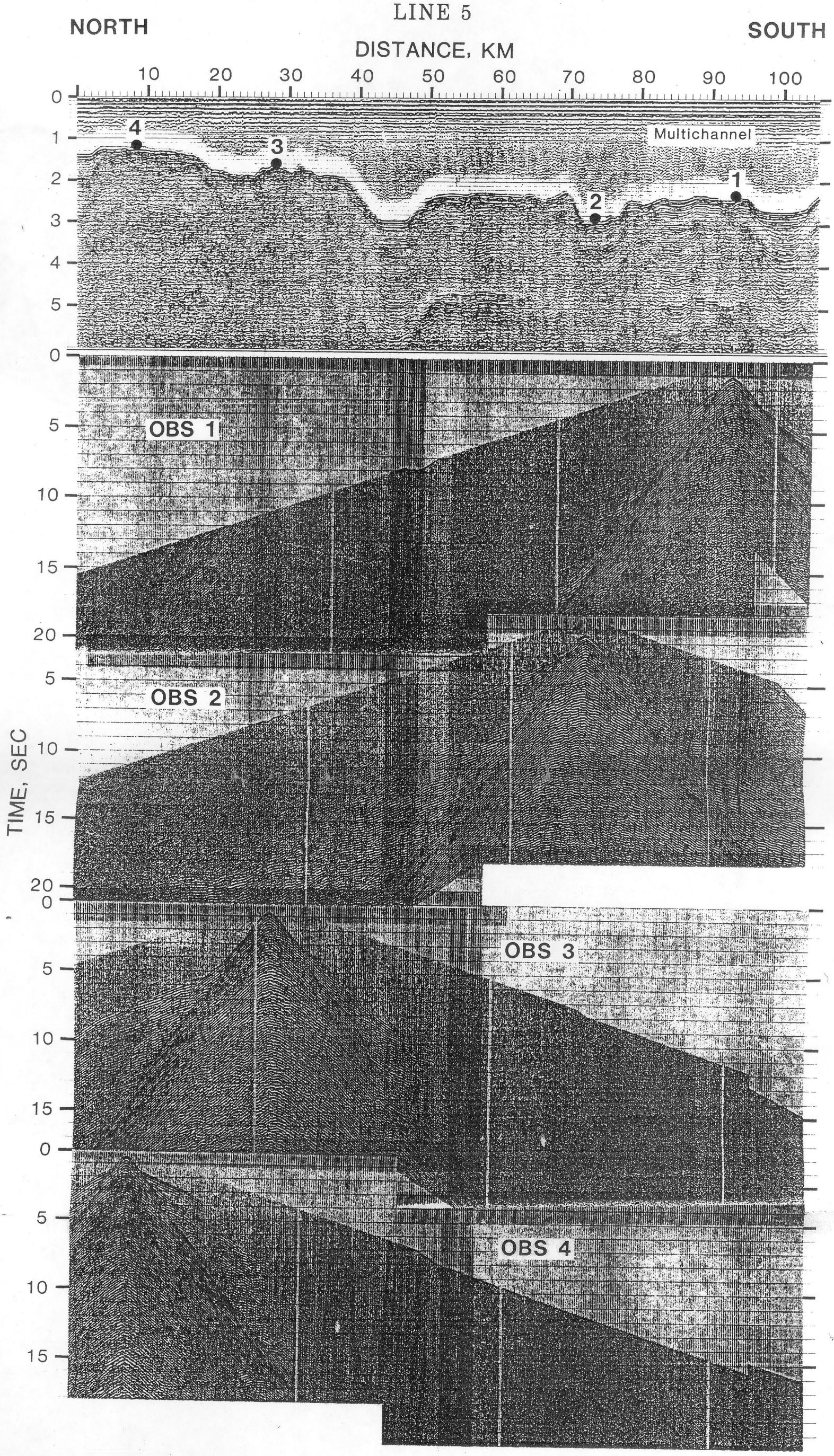
LINE 5
NORTH
SOUTH
DISTANCE, KM
10
20
30
40
50
60
70
80
90
100
Multichannel
1
2
3
4
OBS 1
OBS 2
OBS 3
OBS 4
TIME, SEC
0
5
10
15
20

ANALYSIS AND INTERPRETATION

Analysis Methods

There are several conventional and unconventional methods to use in analyzing and interpreting the kind of seismic data acquired in this experiment. The simplest and most common method for large offset refraction data is the interpretation in terms of flat, constant-velocity layers as calculated from the slope and intercept time of refracted arrivals. If the structure is not too complicated, this method will give a rough estimate of the velocity-depth profile. The method, however, breaks down if there are velocity inversions or if large lateral velocity variations exist.

Near-vertical reflection data can be analyzed using moveout of arrivals with offset as in ordinary reflection work. The larger offsets available in this experiment compared to normal reflection surveys allow us to determine interval velocities more accurately, although the large offsets require us to account for non-hyperbolic moveout.

Since the data acquired in this experiment are of sufficiently high spatial density and since they cover a wide offset range including both pre-critical and post-critical reflections, they can be slant stacked successfully into the tau-p (intercept time vs. ray parameter) domain. The transformed data can be inverted to obtain bounds on the velocity-depth function.

These procedures, however, assume that either the structure is horizontally homogeneous or the lateral variation is at most gradual. Unfortunately, neither assumption is valid for most areas covered in the present experiment since parts of all five lines of the experiment lie over shallow salt structures which exhibit a high degree of lateral heterogeneity. Therefore, we must find some alternative way of analyzing this data set.

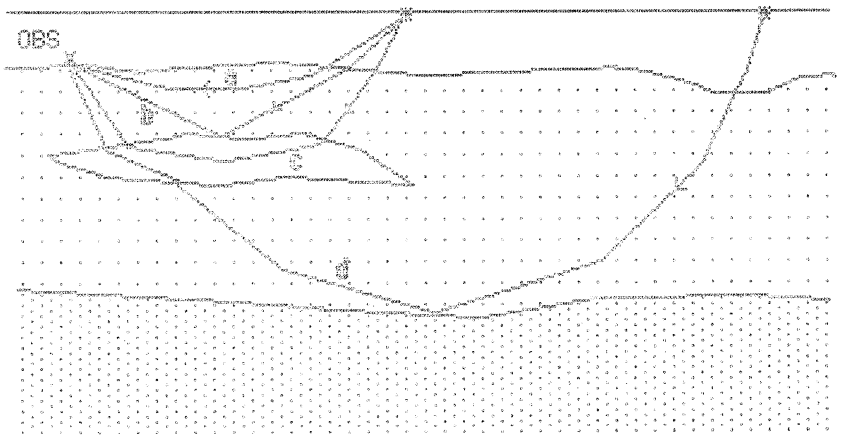

Fig. 5. Seismic rays commonly observed in areas with allochthonous salt: a) refractions and reflections from shallow sedimentary layers; b) reflections from top of salt; c) refractions through upper part of salt; d) refractions and reflections from deeper layers through salt.

The method we have found most successful is two-dimensional (2-D) ray tracing. The procedure we followed can be summarized as follows: a) First, we construct a starting model of the shallow structure near each OBS based on available information including preliminary interpretation as to the identity of the observed arrivals (Fig. 5), standard layered-model interpretation, some geometrical considerations and multi-channel reflection data. b) On this model, shoot a set of rays in reverse, originating at each OBS location and ending at shot points near the sea surface, and compute distance and travel time for each ray. c) Compare the computed travel times with observed travel times, adjust the model accordingly and repeat the procedure until a satisfactory fit is obtained. We also pay attention to any focusing and defocusing of rays, which should be manifested in the observed amplitudes. d) Once a satisfactory near-OBS shallow structure is constructed, shoot another set of rays that penetrate through the shallow structure and appear at large offsets, and compare them with observations to determine the deeper structures.

The following line-by-line interpretations reflect the difference in approach and style of individual interpreters. However, we have tried to preserve consistency among lines, especially when they intersect each other.

Line 1 Interpretation (*cf.* Figs. 4a and 6)

Line 1 is located at the northeast corner of the study area and ties with Line 3 near its northwest end and with Line 4 near its southeast end, Fig. 1. Four OBS's were deployed on this line at water depths ranging from 50 m to 765 m. The subsurface is mostly characterized by a thick low-velocity sediment cover. Near-surface salt is encountered at the sites of OBS's 3 and 4 in the southeast half of the line. No information as to the depth to the basement is obtained.

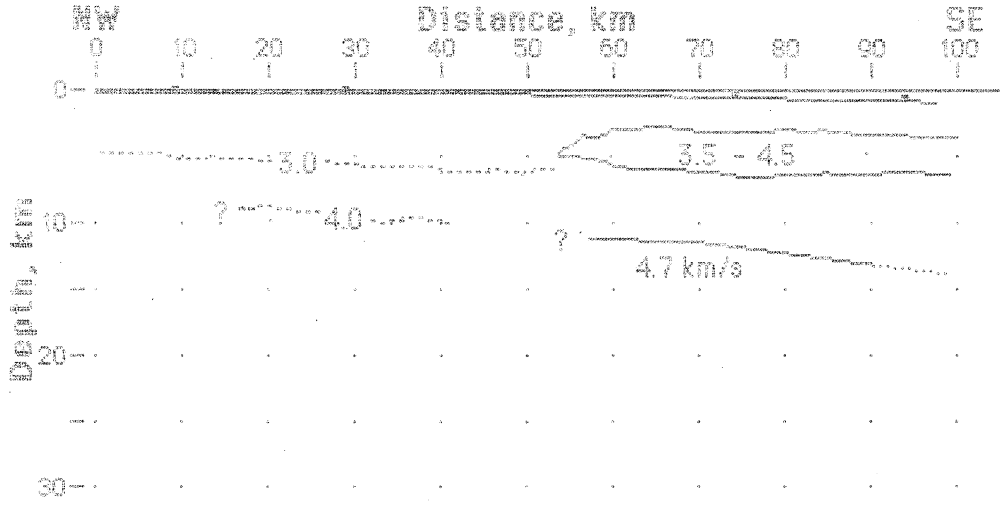

Fig. 6. Line 1 structural profile.

OBS 4 (at 93.9 km): Salt is found at about 3 km depth below the surface. The top-of-salt velocities determined from high amplitude refractions are typically 3.5 km/s. Two-dimensional ray tracing suggests that salt velocities increase with depth to 4.5 km/s and that the thickness of the salt must be 3 to 4 km. Refracted arrivals stop

abruptly, indicating either a velocity inversion or a low velocity gradient in the sediments below the salt extending to great depth. A large amplitude arrival of phase velocity 4.7 km/s is interpreted as a refraction from a layer a few km below the middle Cretaceous unconformity (MCU, *cf.* Line 4 interpretation). Large amplitudes at a limited distance range may indicate existence of a high velocity gradient in this layer. However, near-surface focussing of seismic energy by a lens-shaped high-velocity structure may also explain such an observation.

OBS 3 (at 74.0 km): The thickness and velocities of the salt underneath this OBS appear to be the same as those under OBS 4. The different appearance of the refracted arrivals through the salt as observed at this OBS can readily be explained by an undulating surface of the salt top as is suggested by the multichannel data. The 4.7 km/s arrival comes in two seconds earlier at this OBS than at OBS 4, indicating a significant shallowing of this refractor towards the northwest.

OBS 2 (at 28.9 km): No salt is encountered at this site. Refractions indicate a slow and smooth increase in seismic velocity with depth within a thick sedimentary cover. Velocities reach 3 and 4 km/s at depths of 6 and 9 km, respectively. No arrivals from depths below the MCU can be identified with certainty.

OBS 1 (at 9.0 km): This OBS was deployed in very shallow water. Because of the rough sea at the time of the experiment, seismic records are grossly disturbed by water-wave noise. The seismic velocity reaches 3 km/s at 5 km depth and a further increase up to 3.6 km/s can be traced to a depth of 11 km. No higher velocities are found on this record section. Several arrival sequences of hyperbolic shapes observed on the record sections of OBS 1 and 2 can be interpreted as reflections either from near-surface high-velocity inhomogeneities or from structural features located off the line.
(J.O.)

Line 2 Interpretation (*cf.* Figs. 4b and 7)

Line 2 runs generally north to south and is the most southeasterly line in this study. The line is divided roughly in half by the Sigsbee Escarpment which is the boundary between the upper slope, with water depth of 1000 to 1200 meters, and the lower slope, with water depth of 1900 to 2500 meters. Three OBS's returned data: OBS 1 at 92 km (Fig. 7), OBS 3 at 28 km, and OBS 4 at 8 km. All three recorded shots along the entire line.

The data from OBS 1 were amenable to interpretation by simple flat layer methods. I used a reflection moveout method to obtain a velocity depth function for the layers under that instrument. Clear reflections are observed for interfaces down to the top of the 4.5 km/s layer. The deeper structure under the south end of the line and all of the structure under the north end of the line were obtained by 2-D ray tracing. This seemed to be the only method suited to dealing with the topography of the seafloor and the probable salt structures shallow in the section. My modeling strategy was to establish the structure under the south end of the line using the reflections and refractions on OBS 1. I established the shallow structure under OBS's 3 and 4 using refracted arrivals to infer velocity and the seismic reflection data to infer the shape of the subsurface structures. For the deep structure under the north end of the line I started with the hypothesis that I could extend the deep layers in the south through to the north. I then proceeded to perturb the velocity and depth of those layers in order to maximize the fit between predicted and observed arrivals. This procedure is by no means unique and should be viewed with a healthy dose of skepticism.

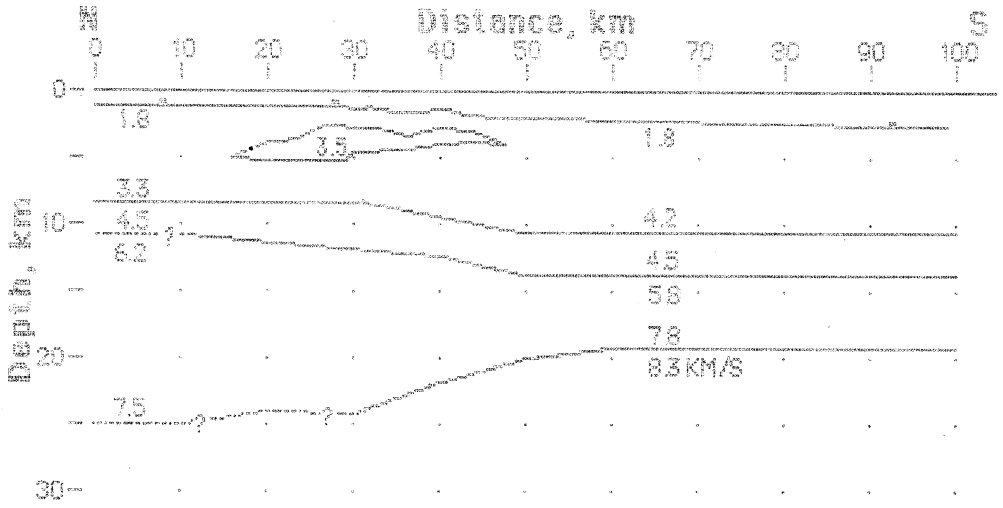

Fig. 7. Line 2 structural profile.

1) 0-15 km: This portion of the line does not seem to be underlain by shallow salt. OBS 4 shows no sign of salt refractions (Fig. 4b), although there could of course be some salt deep enough in the section so that the velocity contrast between salt and clastic sediment is small enough to be missed. The deeper layers under this portion of the line are dashed to indicate that we have not sampled this portion of the subsurface. The boundaries are thus not constrained.

2) 15-45 km: A body of salt varying in thickness from about 1500 meters at 15 km to 3000 meters at 28 km to 0 meters at 45 km underlies this portion of the line. The salt shows up clearly in refracted arrivals on both sides of OBS 3 (Fig. 4b). Its velocity seems to be about 3.5 km/s. This is at the low end of velocities expected for salt and it is possible that the structure on the top of the salt is causing this to appear a little lower than it really is. This pod of salt has a clear low-velocity zone below it that we assume to be clastic sediments. The effect of the low-velocity zone can be seen clearly on the record section for OBS 3 for shots to the south (Fig. 4b). The salt refraction, visible at distances of 32-42 km, terminates as rays are bent down into the low velocity region. I infer the top of the 4.5 km/s layer to be the MCU and to correspond to a boundary between clastic sediment and carbonates. This interface seems to be at about 9 km depth under the upper slope. The basement surface (top of 6.2 km/s layer) seems to be at least several km shallower and perhaps of slightly higher velocity here than under the south part of the line. The Moho is probably dipping down to the north under the upper slope, although there are no rays traveling through the Moho north of about 30 km. The Moho and basement are constrained by arrivals on OBS's 3 and 4 at offsets of 50 to 60 km.

3) 45-100 km: The lower slope, seaward of the Sigsbee Escarpment, is characterized by gently dipping flat layers. There is no sign of salt in the section. The MCU is at a depth of about 11 km, basement is at about 14 km, and the Moho is at about 19 km. The crustal velocities, 5.8 km/s at the top and 7.8 km/s at the bottom, are consistent with those of oceanic crust.
(D.S.S.)

Line 3 Interpretation (*cf.* Figs. 4c and 8)

Line 3 crosses the shelf break from north to south, is 95 km long and has water depths ranging from 47 m at the north end (distance reference) to a maximum depth of 1200 m at 89 km. The line may be divided into three distinct regions by bathymetry: 1) the continental shelf, 0-42 km; 2) the continental slope, 42-89 km; and 3) the region leading to the outer-slope high, 89-95 km. This line ties with Line 1 at the north end and with Line 4 toward the south, Fig. 1.

Except for the extreme southern end of the line, the structure along this line is relatively simple compared with the other four lines. A straightforward inversion of the slopes and intercept times of clear refracted arrivals using a flat-layers model gives seaward-dipping, shallow, sedimentary layers to depths of about 3-4 km. The result of this initial inversion was used as the starting model for 2-D ray tracing. Small depth and velocity perturbations were made to this initial model of the first 3-4 km, and the corresponding travel-time curves from the ray-tracing algorithm were fit to the first 8 sec or so of the data records. This same process was then extended to incorporate the deeper refraction picks until the region had been modeled (Fig. 8) in a fashion to give good agreement with most refracted and reflected arrivals noted in the data records from the four OBS's.

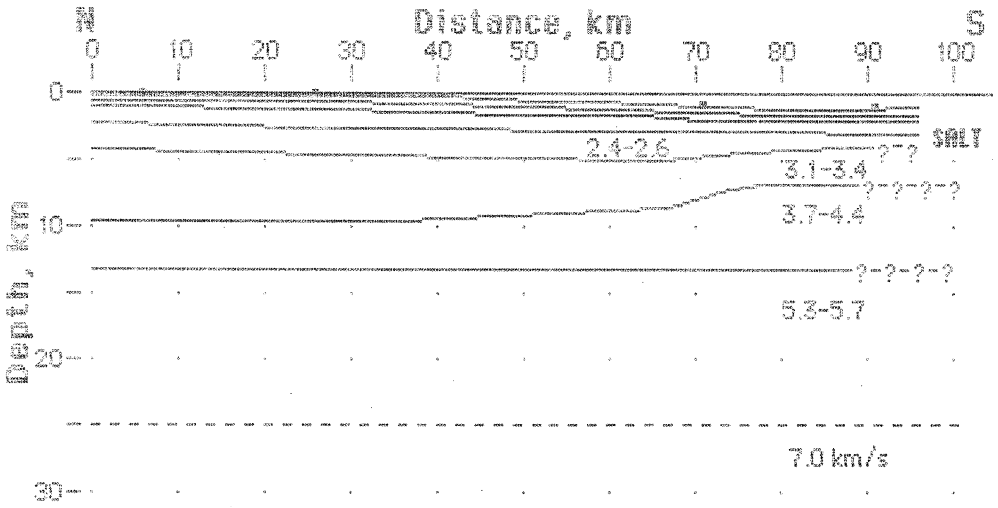

Fig. 8. Line 3 structural profile.

The bathymetric regularity of the first 89 km is found to be reflected also in the deeper parts of the seismic record for this line. The early refracted arrivals of high velocity characteristic of shallow salt intrusions are seen only at the southernmost part of the line, south of OBS 1 (which was located at 91 km on the steepest part of the bathymetric high covered by the line). The primary features of this line are as follows:

1) 0-50 km: The northern half of the line consists of 10 km of sediments (1.7-3.4 km/s) atop a 3-km thick Challenger unit (3.7-4.4 km/s), which in turn is underlain by a flat basement (5.4-5.7 km/s) at 13 km depth. The upper layers generally have a slight seaward dip.

2) 50-89 km: The dip of the upper unconsolidated sedimentary layers slightly increases and tracks the steeper dip of the sea floor, but the deeper sedimentary layers remain relatively horizontal. The Challenger unit becomes thicker and its upper boundary (the MCU) becomes shallower in the seaward direction, rising from a depth of 10 km over the first half of the line to 7 km at 75 km onward. The basement remains flat at 13 km depth with a velocity of 5.3 to 5.4 km/s.

3) 89-95 km: The upper sedimentary layers track the abrupt onset of a bathymetric high, while the deeper layers remain mostly unaffected by this feature. There is strong evidence in the seismic record, however, for shallow high-velocity material (presumably salt) from 90 km onwards, but there are insufficient data to determine the shape or depth of this structure. Inasmuch as the range of possible salt velocities overlaps the range of velocities used to model the Challenger unit for this line, it is also possible that salt pillows with no detectable seismic signatures may exist in the unit toward the southern end of this line.

While it is impossible to pick any Moho arrivals unambiguously on this line, the region below the top of basement (5.3-5.7 km/s at 13 km depth) was modeled by assuming that the velocity increased linearly with depth from the basement surface downwards, and that the velocity was 7.0 km/s at 25 km depth.
(W.P.O.)

Line 4 Interpretation (*cf.* Figs. 4d and 9)

Line 4 is an east-west line that roughly parallels the coast near the shelf break and was collected in 600-800 m of water (Figs. 1, 9). It intersects and completes a triangular grid with Lines 1 and 3. Data from a total of five OBS's were collected along this line.

A standard flat-layer time-distance analysis was used to interpret the sedimentary velocities of the western half of the line. The eastern sedimentary section and crustal arrivals were interpreted by means of 2-D ray tracing because of salt bodies at shallow depths within the sediment column. These deformed the sedimentary strata and caused velocity inversions and lateral velocity inhomogeneities.

By correlation with multichannel data collected and tied to wells in the Mississippi Canyon area, the uppermost strata comprise a thick section of alternating Pleistocene sands and shales. These overlie a zone of approximately the same thickness in which velocities increase relatively slowly with depth, suggesting a mostly fine-grained Neogene section. This is underlain in turn by approximately 2.5 km of strata interpreted as distal turbidites, fine-grained clastics with a significant percentage of pelagic facies, deposited in Upper Cretaceous-early Tertiary time.

There are two structures within these upper units described on the basis of 4.0-4.6 km/s velocities as salt mobilization features. One is a relatively thin lens, the other, a thicker, more disruptive pod. Both are mostly, if not completely, detached. Either may be diapiric or an overthrust feature. The interval designated as the "Challenger Unit" is interpreted on the basis of the 4.0-4.6 km/s velocity. This value is typical of a Jurassic(?)-Lower Cretaceous seismic unit mapped across the deep basin. Its upper boundary in the deep Gulf is interpreted as a middle Cretaceous unconformity (MCU) and its lower boundary as a basement surface. The anticline within this unit is interpreted primarily on a multichannel line acquired along with the OBS data. We

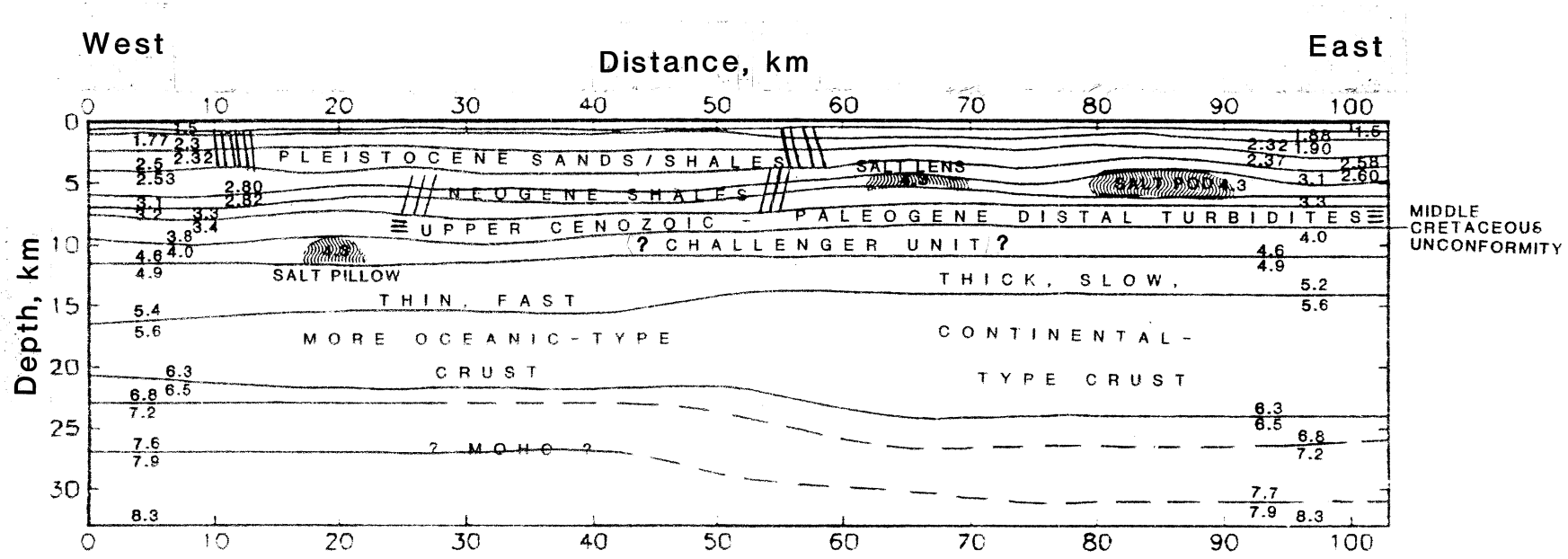

Fig. 9. Line 4 structural profile.

consider it a salt pillow, a minor mobilization feature having, within this unit, no velocity anomaly.

The above interpretations are based on both the literature of coastal-plain subsurface geology and on deep-basin seismic stratigraphy. The gross units interpreted here are seen as thick sedimentary strata connecting the plain with the deep basin section. As a strike line, Line 4 is fairly well situated to allow resolution of these units by means of refraction and wide-angle reflection arrivals.

These sedimentary sections overlie a 5.1-5.2 km/s crustal interval that is deeper in the section to the west than to the east. This fact, plus the presence of high-velocity arrivals on the west, are interpreted as evidence for a relatively thin, deep, fast crust under the western half of the line, and a relatively shallow, thick, slow section of more continental-type crust to the east. The basement structural relief is notable here because it varies along strike. The eastern salt structures, moreover, are preferentially interpreted as salt overthrusts emplaced above a basement structural high. We therefore suggest that basement relief not only controlled the location and thickness of salt deposition but also the type of subsequent salt tectonism, the dominant geologic feature in this area.
(F.J.S.)

Line 5 Interpretation (*cf.* Figs. 4e and 10)

Line 5 is a north-south line located entirely in the mid-slope region of the northern Gulf with very rough bathymetry ranging in depth from 940 to 2270 m. Along its 105 km length, it crosses four major topographic highs with small basins in between. Because of this rough topography and associated large lateral structural variations, 2-D ray tracing was practically the only way to treat the acquired data. The analysis proceeded first to determine the near-OBS sedimentary structure, then to determine the salt structure below, and finally to use this information in interpreting the far-offset arrivals for deeper structures. In the following descriptions, the cited distances are measured from the north end of the line.

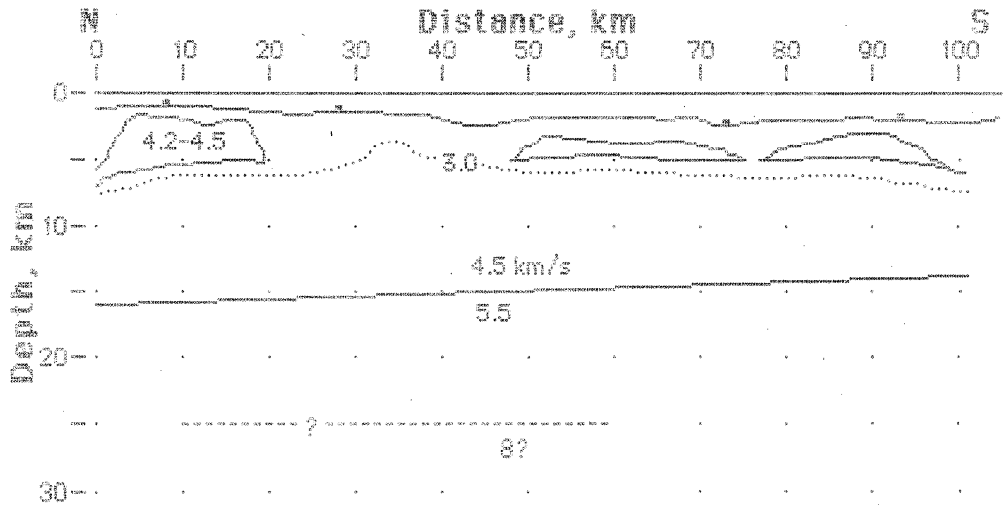

Fig. 10. Line 5 structural profile.

1) 0-20 km: The northernmost 20 km of the line is dominated by a massive salt structure that comes very close to the ocean floor, typically within 1 km. The sediment column above the salt shows compressional-wave velocity increasing from near water-wave velocity (1.5 km/s) to about 2.4 km/s just above the salt. At the top of the salt, the velocity jumps to about 4.2 km, increasing slightly with depth to about 4.5 km/s at the bottom of the salt. The salt is 3 to 4 km thick, with the thicker end towards the north.

2) 25-40 km: In contrast to the topographic high to the north, this topographic high does not contain any appreciable amount of salt. A slight increase in velocity from 2.5 km/s to 3 km/s at a depth of 2.6 to 3 km may indicate existence of very thin or only a trace of salt in this structure.

3) 50-70 km and 80-95 km: These two topographic highs are similar to each other, containing salt extending downward from 3.5 to 4.5 km depth, or about 2 to 3 km below the ocean floor. These salt structures are estimated to be only 1 to 2 km thick. Thus they are considerably deeper and thinner than that at the north end of the line.

4) Deeper arrivals are seen only through isolated 'windows' of efficient seismic transmission. Most of these windows appear in or around basins, where either lesser amount of attenuation and scattering of seismic energy or possible focusing of seismic rays makes these places more efficient in transmitting detectable deep-penetrating signals. Using such arrivals and stripping off the shallow structures as determined above from the data, the depth and velocity of deep-seated layers can be estimated. The arrivals seen on OBS's 1, 2 and 4 from shots above the basin around 45 km from the north end of the line indicate the existence of a major discontinuity in velocity, increasing from 4.5 km/s to 5.5 km/s at about 15 km depth. The difference in intercept times of this arrival at various OBS's indicates that this boundary deepens slightly towards the north. This discontinuity may represent the boundary between the sedimentary column and the crystalline basement below.

5) No clear Moho arrivals are seen on the record sections of this line. However, if we interpret the group of high-energy arrivals seen at far distances on the record section of OBS 2 (the only OBS located in a basin) to be Moho reflection/refraction near critical distance, we can place the depth to the Moho at about 25 km under this line.

Figure 10 schematically shows the inferred structural profile under Line 5. There is considerable variation in the depth to the well-defined top of the salt mass. The base of the salt, in contrast, is not well defined. No reflections from the base of the salt have yet been identified, and its location is only inferred from the lateral extent and delays of various arrivals through the salt layer. For structures below the salt, only approximate depths and general trends can be inferred from the observed data. If our interpretation of isolated distant arrivals is correct, the crust under this line is about 10 km thick. How this thickness varies within this area cannot be determined from the data because the slight downward dip of the top of the basement towards north may or may not be associated with similar or even larger dip at the crust/mantle boundary.
(Y.N.)

Regional Interpretation and Discussion

A total of twenty OBS record sections were obtained from five track lines to study the northern continental margin of the Gulf of Mexico (Fig. 1). Each line was approximately 100 km long. Altogether, the study area covered about 3500 sq nmi

(12,000 km^2) on the upper slope south of Louisiana. The slope here is underlain by a thick sedimentary section that is internally deformed by salt tectonism. The total thickness of sediments and the character and thickness of the crust here have up to now only been loosely constrained by indirect methods. Our study, however, encompasses all components of the shallow geologic record: sediments, salt intrusives and basement character. We discussed above the details of each line individually; here we will present a brief, integrated interpretation of our findings.

The sediment column varies in thickness in this area from 11 to 15 km. Most of this section, the upper 8 - 10 km, consists mainly of Upper Cretaceous - Cenozoic clastics derived from drainage systems in what is now Louisiana and Mississippi. As much as 4 km of the section may be Pleistocene in age.

Despite this great volume of sediments the dominant physiographic feature of the area is salt tectonism. Salt intrusives are interpreted on four out of five lines and were also detected on the extreme southern end of Line 3. These intrusives are, on the whole, thickest in the northern part of the study area, and they thin to the south. They are interpreted as detached, i. e., allochthonous salt bodies. They may be the result of either vertical diapirism or of overthrusting, with lateral as well as vertical transport. There may be a thin stem connecting these bodies to the original depositional strata at depth; these would not be resolvable in our data. What is clear, however, is that they are not vertical stocks. For most if not all of their lateral extent they are underlain by a velocity inversion, presumably in clastic strata. The actual thickness of these intrusives is not clearly observable by means of reflections from the boundary between the salt and the underlying strata. Rather, the thickness is inferred by means of offset ranges over which salt-velocity refractions from a given salt feature can be seen. The longer the offset distance, the thicker the salt.

We have also made an empirical correlation between these data and seismic stratigraphic units in the deep basin that tie to wells on the northeastern Gulf shelf. On the basis of appropriate velocities and depths in section, we interpret here a middle Cretaceous surface. This feature is synchronous with a major turning point in Gulf history; specifically, the transition of the Gulf from a carbonate-bank-rimmed basin to an important clastic depocenter. In our study area, we correlate this surface with the upper boundary of an interval that is variously picked as 4.3 to 4.7 km/s on Lines 1, 2, 4, and 5. On Line 3, the velocity of this interval ranges from 3.7 to 4.4 km/s. The boundary is shallowest, around 7-8 km, at Line 2 north and Line 3 south; it dips north and west to about 10 km and also basinward (Line 2 south) to about 11 km depth.

The basement surface underlying the sediment column is defined here as the top of a crustal section with velocities of at least 4.9 km/s. On Line 2, this boundary dips to the south from 11 to 14 km. On Line 5, this boundary dips to the north from 14 to 16 km. Under the triangular grid, Lines 1, 3 and 4, it is interpreted as having an overall dip to the west from 10.5 to about 12 km. Broadly, the 3-line grid and Line 2 north allow the interpretation of a minor crustal structural high at a depth of about 11-12 km. This high dips basinward (Line 2 south) and westward (Line 5). There is probably some secondary relief on this surface accounting for the northerly dip on Line 5 and the relatively abrupt change in dip on Lines 2 and 4. This data set gives no information about whether this structural high continues to the north beyond Line 3 or to the east.

The crustal section itself is characterized by velocities of 4.9 to about 7.8 km/s. Except at Line 2 south, the crustal thickness varies from about 9 km on Line 5 to at least 15 km on Line 4. The thickness values, combined with a broad velocity range, are best

compared to "transitional" crust: thinned, subsided, modified continental crust often interpreted as underlying continental margins. At Line 2 south a section typical of oceanic crust, 5.5 km thick with velocities ranging from 5.8 to 7.8 km/s, has been interpreted. Line 2 is therefore seen to straddle a transitional/oceanic crustal boundary, defining at least at one point the limit of a possible oceanic-spreading regime.

The lower crustal boundary, with speeds in excess of 7.8 km/s, can be interpreted as being at least 25 km deep on Lines 3 and 4; at about 25 km on Line 5; and at 19 km depth at Line 2 south. The obvious conclusion is that this boundary dips generally landward beneath our study area.

These interpretations are the result of airgun/OBS surveys; specifically, they are attributable to the high sampling density possible when using airgun sources with several receiving units at long apertures on each line. We have, in fact, used such data to define sedimentary units; to resolve the lateral and vertical extent of detached salt bodies; to define a middle Cretaceous surface; and to define the depth, character, and overall trend of basement for the heavily-sedimented, salt-riddled northern Gulf continental slope. We studied here an admittedly small portion of the entire Gulf margin. It is our hope, however, that we can use this, additional existing studies of similar scale, and future projects to map these features comprehensively and better explain the origin and evolution of the Gulf and other basins.

Recommendations for Future Experiments

After this experiment was completed, it was clear that though the experiment was generally successful in revealing many structural features, there also were certain shortcomings. We list below some of these deficiencies and discuss some recommended solutions.

1. Low signal level: Using air guns for seismic signal sources has clear advantages over using explosives in terms of uniformity of source signatures, high spatial density of shot points and high accuracy of shot times. However, the signal level of individual air-gun shots is low compared with those of explosives. This is a clear limitation especially when one desires to record deep refractions through a thick, poorly consolidated sedimentary section similar to what we encountered in this study area. Besides the obvious solution of increasing the capacity of air guns, which is not always feasible technically or economically, there are many ways to improve the observed signal level from air-gun shots.

a) Finding optimum air-gun depth: -- We used 2000 cubic inch air guns towed at a depth of 35 feet for this experiment. This was not only because we normally tow them at this depth for our multichannel work, but also because the bubble-pulse frequency at this depth of towing (about 6 Hz) is near the low end of the instrumental pass band, which is limited by our use of 4.5 Hz geophones. Although low frequency is advantageous for a long-distance transmission of seismic signals, it does not effectively utilize the surface ghost to enhance the emitted signal. Increasing the towing depth is expected to increase the bubble frequency and signal enhancement by ghost, but it also increases transmission loss. However, we have not conducted any controlled experiment to study their overall effect on signal reception at large distances. We recommend that such experiment be done to determine the optimum depth of towing of air guns for wide-offset experiments.

b) OBS location: -- This experiment has revealed that signal strength of deep refractions is highly dependent on the bottom topography and near-surface geology. Deep refractions are generally strong when the shooting ship is over a basin or a region of well-stratified layers, but are very weak over complex salt structures. The cause of this difference may be attributable either to focusing and defocusing of seismic rays by structures or to the difference in absorption and scattering of seismic energy through different geologic structures. Whatever the reason for this difference, we will be better off locating OBS's in basins or over well-stratified structures rather than over complex salt structures whenever possible.

c) Repeated shots: -- Detection of weak seismic signals at far distances is often accomplished by correlation of arrivals across several neighboring traces. Thus, theoretically the higher the spatial density of the sources, the better the chance of detecting weak signals because of the increased effective signal-to-noise ratio. For the present experiment, we shot a part of each line at 50% higher spatial density than the rest. The result, however, is inconclusive. We may need a larger difference in spatial density to see the effect clearly. An extreme case will be to keep the shooting ship stationary while shooting a large number of shots at a given distance. However, we are not ready to recommend this except for experimental purposes because the additional ship time required to achieve appreciable improvement in the signal-to-noise ratio is quite significant and may even be uneconomical.

d) Multiple OBS's at one location: -- The other way to increase the data density for a better signal-to-noise ratio is to deploy more than one OBS at a given location. Assuming that they are separated by a distance sufficient to have independent background noise but close enough to detect essentially the same distant arrivals, we should be able to achieve significant improvement in signal-to-noise ratio.

e) Geophone selection: -- We have not yet conducted any controlled experiment to determine the relative contributions of various possible sources of noise to the overall background noise. If the noise generated at the geophone is significant, and we have a reason to believe it may be, selection of geophones with higher output and larger suspended mass may improve the overall signal-to-noise ratio. We recommend that we examine various possible sources of noise to see if some of them may be controllable.

2. Line geometry: Unless the structure is nearly flat in all directions, the orientation of the shooting line and OBS locations are very important in acquiring readily interpretable data. In general, data from lines parallel to the strike of stratigraphic units , such as Line 4 of this experiment, are easier to interpret than those perpendicular to the strike, which may contain layers with rapidly changing depths. In areas of large lateral heterogeneities, reflections and refractions from features off the shooting line may significantly influence the observation. Fortunately, since each OBS is completely detached from the shooting ship, there is no problem in deploying some OBS's off the shooting line. Off-line OBS's will help remove ambiguities of interpretation due to structural variations perpendicular to the shooting line. If appropriate, non-linear shooting geometry may also be adopted to further enhance the lateral control. For future experiments, it is recommended that due consideration be given to the most appropriate geometry for shooting lines and OBS locations.

3. Data analysis techniques: Though we have found it most successful to use 2-D ray tracing in dealing with complex structures like those found in this study area, the technique is non-unique, and the resulting structure may not be a correct one. One

way to test the validity of the derived structure is to compare synthetic seismograms based on the derived model to the observations. Therefore, we recommend that such an approach be developed for use in future studies.

Conclusions

The air-gun/OBS experiment in the Green Canyon area of the northern Gulf of Mexico, offshore of Louisiana, has revealed that most of the covered area except Line 3 and the northwestern half of Line 1 is underlain by relatively shallow detached salt of seismic P velocity in the range of 3.5 to 4.5 km/s. The thickness of the salt varies from place to place in the range of 1 to 3 km, but a general trend of thinning toward the southern part of the study area is noted. While the top of the salt is well defined, the bottom is not. The root of the salt, if extant, is indistinguishable from high-velocity clastics at depth.

On most lines, the top of the Challenger unit (i.e., MCU) and the top of the presumed basement are identifiable below the salt layer. The basement, which is at about 15 km depth at most places in the study area, appears to be pulled up by a few kilometers beneath the outer slope.

We were not successful in clearly defining the depth to the Moho except in the extreme southern part of the study area, where it deepens from 19 km depth off the Sigsbee Escarpment to about 25 km under the outer slope region. For a clear definition of the sub-basement structures below the thick, poorly consolidated sedimentary cover typical of this area, we need to improve our data acquisition techniques.

Acknowledgements. The ocean-bottom seismographs used for the experiment were designed principally by Paul L. Donoho, now with Gulf Research & Development Co., working under the direction of Gary V. Latham, now with Cities Service. Phillip H. Roper, Paul M. McPherson and Michael Butterfield were responsible for building, maintenance and operation of the instruments as well as many other related mechanical, electronic and programming tasks. Captain Bruce H. Collins of R/V *Fred H. Moore* and his crew were extremely helpful in making this experiment successful. Kenneth H. Griffiths, Jan D. Garmany, Patricia E. Ganey, Subir Chatterjee, George W. Pearcy, Stirling Gilfillan and Oscar Febres-Cordero were responsible for many ship-related operations including electronics, mechanical work, navigation, data acquisition and communication. The 2-D ray tracing program used in this study was developed by Kevin MacKenzie based on the original program of V. Cerveny.